Protonation State of Methyltetrahydrofolate in a Binary Complex with Cobalamin-Dependent Methionine Synthase †

ARTICLE *in* BIOCHEMISTRY · DECEMBER 2000

Impact Factor: 3.02 · DOI: 10.1021/bi001431x · Source: PubMed

2 AUTHORS:

April E Bednarski
Washington University in St. Louis
16 PUBLICATIONS **305** CITATIONS
SEE PROFILE

Rowena Green Matthews
University of Michigan
172 PUBLICATIONS **13,331** CITATIONS
SEE PROFILE

Protonation State of Methyltetrahydrofolate in a Binary Complex with Cobalamin-Dependent Methionine Synthase†

April E. Smith‡ and Rowena G. Matthews*,§

Departments of Medicinal Chemistry and Biological Chemistry and Biophysics Research Division, The University of Michigan, Ann Arbor, Michigan 48109-1055

Received June 22, 2000; Revised Manuscript Received August 14, 2000

ABSTRACT: *N*5-Methyltetrahydrofolate (CH_3-H_4folate) donates a methyl group to the cob(I)alamin cofactor in the reaction catalyzed by cobalamin-dependent methionine synthase (MetH, EC 2.1.1.3). Nucleophilic displacement of a methyl group attached to a tertiary amine is a reaction without an obvious precedent in bioorganic chemistry. Activation of CH_3-H_4folate by protonation prior to transfer of the methyl group has been the favored mechanism. Protonation at N5 would lead to formation of an aminium cation, and quaternary amines such as 5,5-dimethyltetrahydropterin have been shown to transfer methyl groups to cob(I)alamin. Because CH_3-H_4folate is an enamine, protonation could occur either at N5 to form an aminium cation or on a conjugated carbon with formation of an iminium cation. We used ^{13}C distortionless enhancement by polarization transfer (DEPT) NMR spectroscopy to infer that CH_3-H_4folate in aqueous solution protonates at N5, not on carbon. CH_3-H_4folate must eventually protonate at N5 to form the product H_4folate; however, this protonation could occur either upon formation of the binary enzyme−CH_3-H_4-folate complex or later in the reaction mechanism. Protonation at N5 is accompanied by substantial changes in the visible absorbance spectrum of CH_3-H_4folate. We have measured the spectral changes associated with binding of CH_3-H_4folate to a catalytically competent fragment of MetH over the pH range from 5.5 to 8.5. These studies indicate that CH_3-H_4folate is bound in the unprotonated form throughout this pH range and that protonated CH_3-H_4folate does not bind to the enzyme. Our observations are rationalized by sequence homologies between the folate-binding region of MetH and dihydropteroate synthase, which suggest that the pterin ring is bound in the hydrophobic core of an $\alpha_8\beta_8$ barrel in both enzymes. The results from these studies are difficult to reconcile with an S_N2 mechanism for methyl transfer and suggest that the presence of the cobalamin cofactor is important for CH_3-H_4folate activation. We propose that protonation of N5 occurs after carbon−nitrogen bond cleavage, and we invoke a mechanism involving oxidative addition of Co^{1+} to the N5−methyl bond to rationalize our results.

Cobalamin-dependent methionine synthase from *Escherichia coli* **(**MetH or methyltetrahydrofolate:homocysteine methyltransferase; EC 2.1.1.3) catalyzes the methylation of homocysteine with methyl groups derived from CH_3-H_4-folate; its cobalamin prosthetic group serves as an intermediary in the methyl transfer. During turnover, the methylcobalamin form of the enzyme is demethylated by homocysteine, forming cob(I)alamin and methionine. The cob(I)alamin cofactor is then remethylated by CH_3-H_4folate, forming methylcobalamin and H_4folate (*1*). Each substrate is bound to a defined module of this 1227 amino acid polypeptide (*2*), and the enzyme-bound cobalamin cofactor must interact with each substrate in turn.

The N-terminal module binds homocysteine and activates it for nucleophilic attack on methylcobalamin (*3*). This module, MetH(2−353), has been separately expressed and purified. MetH(2−353) exhibits homology with betaine: homocysteine methyltransferase (*3*, *4*), an enzyme that catalyzes methyl transfer from a quaternary amine to homocysteine without the assistance of any organic cofactor.

Residues 353−649 form a module that binds and activates CH_3-H_4folate. This module shows significant sequence homology to AcsE, a methyltransferase from *Clostridium thermoaceticum* (*5*). AcsE binds CH_3-H_4folate and catalyzes methyl transfer from CH_3-H_4folate to the corrin of a separate protein, AcsD, in the Wood−Ljungdahl CO_2-fixation pathway (*6*, *7*). MetH(353−649) also has sequence homology with two other methyl transfer enzymes: MtrH from *Methanobacterium thermoautotrophicum* (*8*) and CmuB from *Methylbacterium* sp. strain CM4 (*9*). MtrH transfers methyl groups from methyltetrahydromethanopterin to the cob(I)-amide form of MtrA; both MtrH and MtrA form part of a membrane-associated multienzyme complex responsible for methylation of coenzyme M (ethanethiol sulfonate) in support

† This work was supported in part by National Institutes of Health Research Grant GM24908 (R.G.M.) and Pharmacological Sciences Training Grant T32 GM007767 (A.E.S.).

* To whom correspondence should be addressed. E-mail rmatthew@umich.edu. Tel (734) 764-9459. Fax (734) 764-3323.

‡ Department of Medicinal Chemistry.

§ Department of Biological Chemistry and Biophysics Research Division.

[1] Abbreviations: MetH, methionine synthase; CH_3-H_4folate, 5-methyltetrahydrofolate; H_4folate, tetrahydrofolate; MES, 2-(*N*-morpholino)-ethanesulfonate; AMT, buffer containing acetic acid, 2-(*N*-morpholino)-ethanesulfonate (MES), and triethanolamine; DEPT, distortionless enhancement by polarization transfer; DHPS, dihydropteroate synthase; AcsE, methyltetrahydrofolate:corrinoid Fe/S protein methyltransferase; CH_3-H_4PteGlu$_1$, 5-methyltetrahydropteroyl monoglutamate; CH_3-H_4-PteGlu$_3$, 5-methyltetrahydropteroyl triglutamate; H_4PteGlu$_3$, tetrahydropteroyl triglutamate.

10.1021/bi001431x CCC: $19.00
Published on Web 10/14/2000

of methanogenesis (*10*). CmuB is a corrinoid-containing protein that catalyzes methyl transfer from chloromethane to tetrahydrofolate (*11*). We expect that MetH(353−649), AcsE, MtrH, and CmuB have similar three-dimensional structures and employ similar mechanisms to activate their methyltetrahydropterin substrates.

The third module of methionine synthase, MetH(650−896), binds the cobalamin prosthetic group (*12*). An X-ray structure of this module has been determined (*12*), revealing that the dimethylbenzimidazole nucleotide substituent of the corrin ring, which provides the lower axial ligand to cobalt in free methylcobalamin, has been replaced by a histidine ligand from the protein. All of the corrinoid proteins involved in the methyl transfer reactions discussed above, AcsD, MtrA, and CmuB, bind cobalamin with the dimethylbenzimidazole ligand displaced. AcsD shows the spectral properties of a five-coordinate methylcobalamin, with no ligand in the lower axial position (*13*), while MtrA (*14*) and CmuB (*9*) have histidine ligands derived from the protein in the lower axial position.

The C-terminal module of methionine synthase, MetH-(897−1227), is involved in reactivation of the enzyme when the cob(I)alamin prosthetic group becomes oxidized to cob-(II)alamin during turnover (*15*−*17*). Activation requires a reductive methylation of cob(II)alamin, in which electrons are provided by reduced flavodoxin and the methyl group is donated by AdoMet, which is bound to the C-terminal domain of MetH. Thus far, this module appears uniquely in methionine synthase enzymes.

The two substrate-binding modules can be expressed as a MetH(2−649) fragment (*2*). Although the MetH(2−649) fragment does not contain the cobalamin binding region, it still is able to catalyze methyl transfer to homocysteine when supplied with exogenous methylcobalamin and also catalyzes methyl transfer from CH_3-H_4folate to exogenous cob(I)-alamin. The rate constants for catalysis of these reactions by MetH(2−649) are identical to those for the MetH(2−1227) holoenzyme, when the holoenzyme reacts with exogenous cobalamin under the same conditions (*2*). In addition, MetH(2−649) has recently been found to catalyze turnover when supplied with separately expressed and purified MetH-(649−1227); the rate of turnover is first-order in each component and characterized by a rate constant of ~50 000 M^{-1} s^{-1} (Vahe Bandarian and Rowena Matthews, unpublished data). Thus MetH(2−649) is highly active in catalysis of the homocysteine and methyltetrahydrofolate half-reactions.

The two methyl transfer reactions that comprise the turnover cycle of MetH have generally been assumed to proceed by S_N2 mechanisms. The overall methyl transfer from CH_3-H_4folate to homocysteine catalyzed by MetH proceeds with retention of stereochemistry at the transferred methyl group, in agreement with the expectation for a double displacement mechanism requiring two successive inversions of chirality (*18*). Cob(I)alamin is an excellent nucleophile, some 40 000-fold more reactive toward methyl iodide than benzylthiolate (*19, 20*). The H_4folate anion is, however, an extremely poor leaving group, so that CH_3-H_4folate must be activated prior to nucleophilic displacement of the methyl group, presumably by protonation of N5. Model studies show that a 5,5-dimethyltetrahydropterin can serve as a methyl donor to cob(I)alamin (*21, 22*), and by analogy we expect that formation of an aminium or iminium cation at N5 could serve to activate CH_3-H_4folate. CH_3-H_4folate binds MetH in its unprotonated form at pH 7.4, and the affinity of the enzyme for CH_3-H_4folate does not decrease appreciably as the pH is lowered to 5.5 (*23*). However, these studies do not preclude an internal proton transfer between a general acid catalyst in the protein and bound CH_3-H_4folate. While protonation at N5 is required to form the H_4folate product, it could occur either in the binary enzyme−CH_3-H_4folate complex, during methyl transfer, or on departure of the H_4-folate product from the enzyme.

Protonation of CH_3-H_4folate in solution is associated with a pK_a of 5.05 as measured by fluorescence spectroscopy (*24*). However, since N5 is the nitrogen of an enamine, protonation might occur either on the nitrogen (N5) or on carbon (C8a or C2) (Chart 1). The position of CH_3-H_4folate protonation

Chart 1

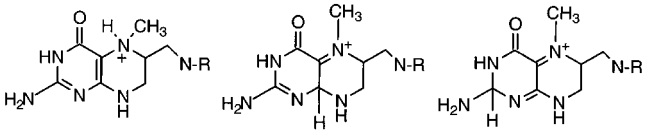

in solution had not been determined previously. DEPT NMR experiments described in this paper show that protonation does not occur at C8a or C2 in solution and support N5 protonation. Furthermore, we also show that CH_3-H_4folate is not protonated in the binary enzyme−CH_3-H_4folate complex, suggesting that protonation at N5 must occur at a later step in the reaction sequence. We present a mechanistic proposal for the methyl transfer from CH_3-H_4folate to cob-(I)alamin that is consistent with our observations.

EXPERIMENTAL PROCEDURES

Materials. $PteGlu_3$ was purchased from Schircks Laboratories (Jona, Switzerland). (6*S*)-CH_3-H_4folate and (6*S*)-H_4-folate were the kind gift of Eprova (Schaffhausen, Switzerland). Phenol red dye was obtained from Sigma, as was chicken liver dihydrofolate reductase.

Synthesis and Purification of (6S)-H_4PteGlu$_3$. CH_3-H_4-$PteGlu_3$ and $H_4PteGlu_3$ were synthesized from $PteGlu_3$ as previously described (*25*). The original procedure employed dihydrofolate reductase from *Lactobacillus casei*, which can reduce $PteGlu_3$ directly to $H_4PteGlu_3$; the procedure was altered slightly to allow for the use of chicken liver dihydrofolate reductase, which is commercially available but which does not reduce $PteGlu_3$ to $H_2PteGlu_3$ (*26*). The $PteGlu_3$ was first reduced to $H_2PteGlu_3$ with sodium dithionite (*27*). $H_2Pte(Glu)_3$ was precipitated by slow addition of 5 mL of 1 M HCl, and the precipitate was collected by centrifugation and redissolved in 10 mM Tris-HCl buffer, pH 7.2, containing 10 mM 2-mercaptoethanol. Chicken liver dihydrofolate reductase (5 units) was incubated overnight at room temperature with the $H_2PteGlu_3$ and 1 mM NADPH to form (6*S*)-$H_4PteGlu_3$. $H_4PteGlu_3$ was purified as previously described (*25*).

Construction of Mutations of MetH(2−649). Aspartate to asparagine mutations were introduced by overlap extension PCR as previously described (*2*). The primers used to make the mutation Asp399Asn were as follows: (coding) 5′-GGCGCGCAGATTATCAATATCAACATGGATG-3′ (nt

1180−1210); (noncoding) 5′-CATCCATGTTGATATTGA-TAATCTGCGCGCC-3′ (nt 1210−1180). The nucleotide (nt) numbering is that shown in the GenBank sequence J04975 of *metH* (*28*). Altered bases are underlined. In the Asp399Asn mutation, the underlined base change at nt 1195 removed the *Cla*I restriction site; loss of the site was used to screen the recombinant plasmids for the mutation. The primers used to construct the Asp434Asn mutation were as follows: (coding) 5′-GTGCCGATTATGATCAACTCCTCAAAATGG-3′ (nt 1285−1314); (noncoding) 5′-CCATTTTGAGGAGT-TGATCATAATCGGCAC-3′ (nt 1314−1285) The base change at 1295 introduced a new *Bcl*I restriction site, which was used in screening recombinant plasmids for the mutation. The Asp522Asn MetH(2−649) was prepared with the following primers: (coding) 5′-GCCAGAAGATATAATAT-TCAACCCAAACATCTTCGC-3′ (nt 1546−1581); (non-coding) 5′-GCGAAGATGTTTGGGTTGAATATTATA-TCTTCTGGC-3′ (nt 1581−1546). Two silent changes were introduced at 1558 and 1561, which provided a screen for the mutation by introducing an *Ssp*I restriction site. The third mutation, at 1565, generated the Asp522Asn mutation. Once the desired fragment was produced by PCR, the fragment was cloned into an expression plasmid pCWG-02 (*2*) containing the wild-type *metH* gene with dual stop codons at 1270−1276. Both the PCR fragment and the expression plasmid were cut with the unique restriction enzymes *Apa*I and *Dra*III to construct the Asp399Asn and Asp434Asn mutations and with *Cla*I and *Dra*III to construct the Asp522Asn mutation. The cut plasmids were gel-purified, combined with the cut PCR fragments, and ligated by previously described procedures (*2*). Sequences of the mutant expression plasmids were confirmed with restriction enzyme assays and by DNA sequencing at the University of Michigan Sequencing Core Facility.

Expression and Purification of MetH(2−649) Wild-Type and Mutant Fragments. Construction and characterization of the overexpression plasmid pCWG02 for production of the wild-type MetH(2−649) has been described, as has the purification of the overexpressed recombinant fragment (*2*). However, a slightly altered enzyme purification method was used in this study. The cells were grown, pelleted, and sonicated as described previously, but no protease inhibitors were added to the sonicated cells. Only one column, an anion-exchange Q-Sepharose gravity-flow column (Pharmacia), was used for purification. MetH(2−649) can be purified to apparent homogeneity in a single chromotographic step due to the very high expression level of this fragment. Enzyme purity was determined by SDS−PAGE, and enzyme concentration was determined by a Bradford protein assay (Bio-Rad).

Assays for Catalytic Activity of MetH(2−649). Methylcobalamin:homocysteine and CH_3-H_4folate:cob(I)alamin methyltransferase assays were performed as previously described (*29*). Briefly, methylcobalamin:homocysteine methyltransferase activity was monitored spectrophotometrically at 37 °C by following the demethylation of methylcobalamin at 525 nm under anaerobic conditions. CH_3-H_4folate:cob(I)alamin methyltransferase activity was measured with radioactive [*methyl* -^{14}C]CH_3-H_4folate by monitoring formation of [*methyl*- ^{14}C]cobalamin.

^{13}C-DEPT NMR Spectroscopy. (6*S*)-CH_3-H_4folate, labeled with ^{13}C at natural abundance, was dissolved to a final concentration of 20 mM in 100 mM potassium phosphate buffer at pH values ranging from 4 to 8. The pH was adjusted as needed with HCl or NaOH. Approximately 4% D_2O was included as the lock signal. ^{13}C spectra were taken on a 300 MHz Varian NMR spectrometer at 25 °C using the 135° DEPT pulse sequence (*30*). Chemical shifts are expressed in parts per million (ppm) relative to tetramethylsilane and were determined with reference to the internal standard methanol (10 mM CH_3OH). The C6 and N5-CH_3 shift data were analyzed by plotting the change in chemical shift in ppm ($\Delta\delta$) as the pH is lowered and fitting the data to eq 1 to obtain the pK_a associated with the shift. In this equation, b_H represents the maximum shift in ppm at low pH (*31*)

$$\Delta\delta = \frac{b_H 10^{(pH-pK_a)}}{1 + 10^{(pH-pK_a)}} \quad (1)$$

Determination of Proton Release/Uptake Associated with Substrate Binding. We employed a previously described method for detecting proton uptake or release on substrate binding using the pH indicator dye phenol red (*32*). These experiments were performed with 50 μM MetH(2−649) in 50 mM potassium phosphate buffer, pH 7.2, and 100 μM KCl at 25 °C. The pK_a for phenol red was determined to be 7.6 under these conditions. The experiments were performed at pH 7.5−7.7 in order to observe maximal changes in the absorbance of phenol red as the pH of the solution changed.

Determination of the Absorbance Changes Associated with Binding of CH_3-H_4Folate and H_4Folate to MetH(2−649) or Introduction of Folate Substrates into Hydrophobic Solvents. Experiments were performed in matched Yankelov (double sector) cells and a double-beam Cary 300 Bio spectrophotometer. All experiments were performed with MetH(2−649) and the pure 6*S* isomer of either CH_3-H_4folate or H_4folate. The buffer used for these titrations, AMT (50 mM acetic acid, 50 mM MES, and 100 mM triethanolamine), was chosen because the ionic strength is constant over the pH range from 5 to 9, as previously reported (*33*). The pH of the AMT buffer was adjusted with 10 M NaOH. Both cuvettes contained enzyme, 10−20 μM, in the front sector and an equal volume of buffer in the back sector. A stock solution of CH_3-H_4folate or H_4folate (3−10 mM) was added to the front compartment of the sample cuvette and the back compartment of the reference cuvette. An equal volume of buffer was added to the front compartment of the reference cuvette. Titrations were performed in air-saturated solutions. H_4folate oxidation was not observed, as assessed by examination of UV spectra during the short time span (5 min) of these experiments.

Difference spectra were recorded for CH_3-H_4folate under acidic and neutral conditions in both aqueous and hydrophobic solvents. The reference cuvette contained AMT buffer, pH 7.2, in both compartments, while the sample cuvette contained AMT buffer, pH 3, in both compartments. Then CH_3-H_4folate (10 μM final) was introduced into the front compartment of both cuvettes and a spectrum was taken. The stock solution of 3 mM CH_3-H_4folate was prepared in AMT buffer, pH 7.2. For the acetonitrile difference spectra, the same method was followed, but 10 μM CH_3-H_4folate was mixed with 80% acetonitrile and 20% AMT buffer, pH 3 (sample) or 7.2 (reference).

Spectral Simulations of MetH(2−649) Binding to CH_3-H_4Folate as a Function of pH. Difference spectra were simulated for CH_3-H_4folate binding to MetH(2−649) at pH values ranging from 5 to 9 to clarify the origin of the observed absorbance changes. For these simulations, the spectra for free CH_3-H_4folate in AMT buffer, pH 7.2 and 3, were used in calculating the spectra for free unprotonated or protonated CH_3-H_4folate, respectively. We assumed that the spectrum of bound CH_3-H_4folate was independent of the solution pH and used the spectrum determined at pH 7.2 in AMT buffer for binding of 12 μM CH_3-H_4PteGlu_3, which binds more tightly than the monoglutamate, with 10 μM MetH(2−649). Difference spectra were calculated for the pH values 5.4 and 5.7. Under these conditions, it has been determined that 95% of CH_3-H_4PteGlu_3 is enzyme-bound (data not shown). The pK_a of 5.05 for protonation at N5 of CH_3-H_4folate was used to determine that 36% of free CH_3-H_4folate would be protonated at pH 5.4 and 18% of free CH_3-H_4folate would be protonated at pH 5.7. With these assumptions, we were able to calculate the spectra of the bound and free CH_3-H_4folate in the sample cuvette and subtract the calculated spectrum of the free CH_3-H_4folate in the reference cuvette to obtain the difference spectrum for CH_3-H_4folate binding to MetH(2−649) at pH 5.4 and 5.7.

Determination of CH_3-H_4Folate Binding by Equilibrium Centrifugation Assay. Rapid centrifuge filtration was used to measure a K_d for CH_3-H_4folate binding to MetH(2−649) (*34*) at pH 7.2. A stock solution of (6*R,S*)-[*methyl* -^{14}C]CH_3-H_4folate was dissolved in 8 mM sodium ascorbate. [*methyl* -^{14}C]CH_3-H_4Folate (0−300 μM) was mixed with 20 μM enzyme, and the mixture was centrifuged in a Microcon filtration unit (Millipore) with a cutoff of 50 kDa. This filtration unit allowed unbound [*methyl* -^{14}C]CH_3-H_4folate to pass through the filter, but all the enzyme was retained. Aliquots of the top and bottom solutions were taken and the concentration of ^{14}C in each fraction was measured in a scintillation counter. The concentration of bound substrate ([ES]) was determined by subtracting the counts per minute (cpm) due to free substrate in the bottom fraction from the cpm due to free and bound substrate in the top fraction. A control experiment lacking enzyme was performed in order to establish that the [*methyl*-^{14}C]CH_3-H_4folate was not retained by the filter. The data were analyzed by plotting [ES] vs $[S]_t$, the total substrate concentration, and fitting the curve to the quadratic binding eq 2 (*35*) to obtain a K_d for CH_3-H_4folate binding:

$$[ES] = \frac{([E]_t + [S]_t + K_d) - \sqrt{([E]_t + [S]_t + K_d)^2 - 4[E]_t[S]_t}}{2} \quad (2)$$

RESULTS

Determination of the Site of Protonation of CH_3-H_4Folate by DEPT NMR Spectroscopy. CH_3-H_4Folate in aqueous solution has a pK_a of 5.05 associated with the protonation of N5, as detected by measurement of fluorescence changes as the pH is lowered (*24*). Since N5 of CH_3-H_4folate is the nitrogen of an enamine, protonation could occur either on the nitrogen or on a conjugated carbon (C8a or C2). To determine where free CH_3-H_4folate protonates at low pH values, a ^{13}C-DEPT 135 NMR pulse sequence was used (*30*) with a sample of CH_3-H_4folate labeled at natural abundance with ^{13}C. In a DEPT 135 experiment, magnetization transfer occurs between hydrogens and the ^{13}C carbon to which they are attached. Carbons lacking a hydrogen substituent are not seen in a DEPT 135 NMR experiment. The DEPT 135 pulse sequence results in an inversion of the methylene carbon signals with respect to the methyl and methenyl carbons.

The NMR spectra shown in Figure 1 were obtained with (6*S*)-CH_3-H_4folate in aqueous potassium phosphate buffer ranging in pH from 3.9 to 8.0. At neutral pH, the ^{13}C chemical shifts compared well with the published chemical shifts for CH_3-H_4PteGlu_1 (*36*). Changes in the resonances ($\Delta\delta$ in ppm) were plotted versus pH for analysis (Figure 2). A downfield shift of 2.4 ppm for the CH_3-N5 signal was observed as the pH was lowered, indicating development of positive charge near the methyl group, e.g., due to protonation of N5. The pK_a for this shift is 5.3 ± 0.1, which is close to the published pK_a value (5.05) for protonation of CH_3-H_4folate (*24*). A similar downfield shift was observed for the C6 signal, which is also consistent with protonation at N5. We would expect protonation on C8a or C2 to result in the appearance of a methine peak with a chemical shift of 40−90 ppm relative to tetramethylsilane (*37*). Therefore, if C8a or C2 were protonated at low pH, a methine signal would be detected that would disappear as the sample pH was raised. No new signal was seen even at pH 3.9, indicating that neither C8a nor C2 was being protonated under these conditions. These results indicate that CH_3-H_4-folate in aqueous solution protonates primarily at N5 rather than at C8a or C2. The next question we wanted to address was whether CH_3-H_4folate was protonated upon binding MetH, and conversely, whether H_4folate was deprotonated upon binding.

H_4Folate Does Not Release a Proton to Solution When Binding to MetH(2−649). CH_3-H_4Folate must protonate at N5 during its conversion to H_4folate. This protonation could occur either upon binding to MetH to form an enzyme−CH_3-H_4folate binary complex, during methyl transfer, or upon release of H_4folate to solution. By use of the pH indicator dye phenol red and a weakly buffered enzyme solution, it is possible to detect micromolar changes in proton concentration as a folate substrate is titrated into a solution containing MetH. It has previously been shown that binding of CH_3-H_4folate to MetH at pH 7.6 does not result in proton uptake from or release to solution (*32*).

We have now examined H_4folate binding to MetH(2−649) using the same method. In this experiment, the enzyme was titrated with (6*S*)-H_4PteGlu_3 in the presence of phenol red at pH 7.6. No proton release to or uptake from solution was detected as H_4PteGlu_3 was titrated into a solution containing MetH(2−649) (data not shown). The results from these experiments show that neither CH_3-H_4folate nor H_4Pte$(Glu)_3$ releases or takes up a proton from solution upon binding to MetH at pH 7.6. Protonation of bound CH_3-H_4folate or deprotonation of bound H_4folate could, however, occur by proton transfer within the enzyme active site without release or uptake of a proton to/from solvent. The next series of experiments was designed to assess this possibility.

UV/Visible Absorbance Changes Associated with Binding of CH_3-H_4Folate to MetH(2−649). When CH_3-H_4folate binds MetH(2−649) at pH 7.2, there is a slight red shift in the

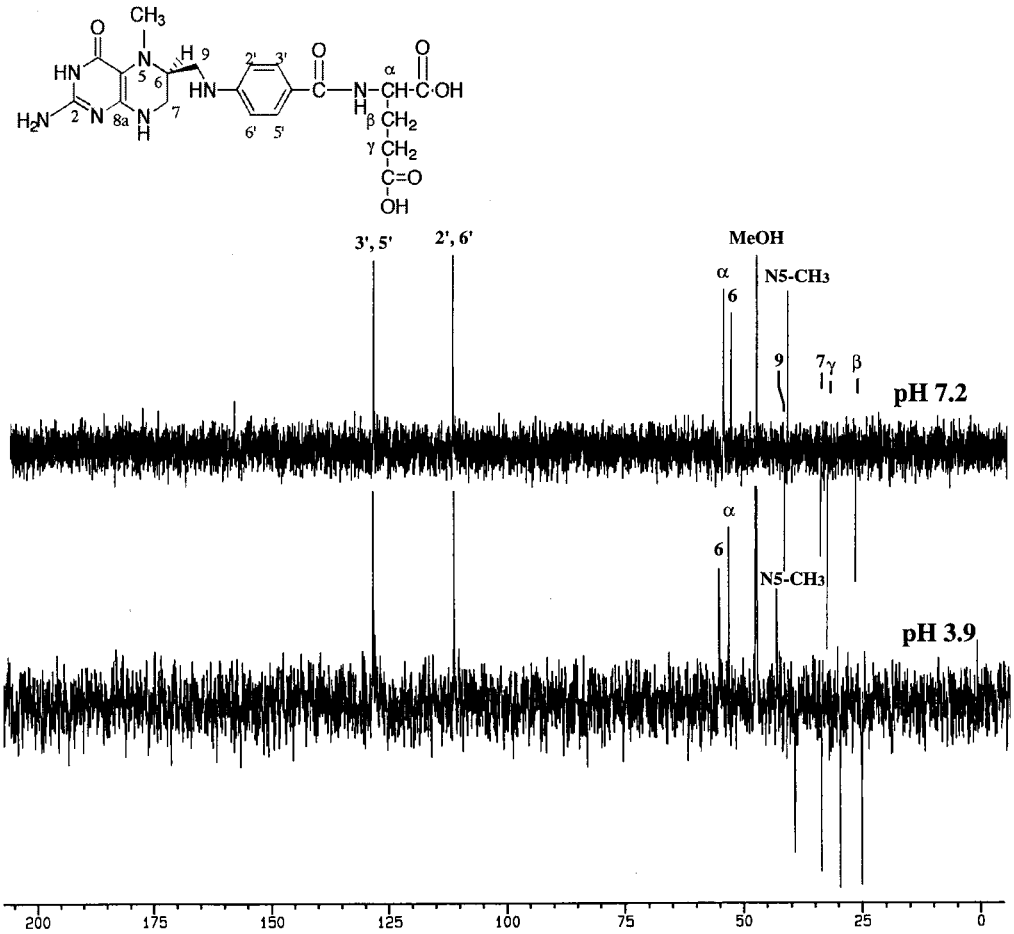

FIGURE 1: ^{13}C-DEPT-135 NMR spectra at pH 7.2 (top) and pH 3.9 (bottom), with the CH_3-H_4folate numbering system shown above the spectra. Peaks are reported as chemical shifts in parts per million (ppm, δ) with respect to tetramethylsilane, and positions were assigned by comparison with the internal standard methanol. Assignments at pH 7.2 were made by comparison with previous published data (*36*), while the assignments at pH 3.9 could be inferred from incremental shifts as the pH was lowered.

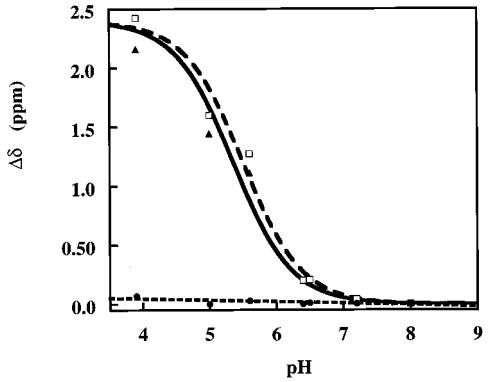

FIGURE 2: Chemical shift changes associated with protonation of CH_3-H_4folate. ^{13}C-DEPT NMR spectra of CH_3-H_4folate at pH 3.9−8.0 show a downfield shift of 2.4 ppm for the N5 methyl group as CH_3-H_4folate protonates (▲) (pK_a of 5.3 ± 0.1). The chemical shift of C6 (□) also shifts downfield by 2.4 ppm as the pH is lowered. By comparison, there is no change in chemical shift for the peak associated with C3′ and C5′ as the pH is lowered (●).

UV absorption spectrum of CH_3-H_4folate, giving rise to a difference spectrum (bound − free) with an absorbance maximum at 308 nm and a molar absorbance coefficient of 4300 M^{-1} cm^{-1} (Figure 3). The absorbance at 308 nm increases with increasing CH_3-H_4folate concentration in a saturable fashion. The K_d for CH_3-H_4folate binding to MetH at pH 7.2 was determined by equilibrium centrifugation binding to be 9 μM, and because this value is smaller than the concentration of enzyme (20 μM) used in measuring the absorbance changes associated with binding, binding is almost stoichiometric in the initial stages of the reaction.

The absorbance changes associated with introduction of neutral aqueous solutions of CH_3-H_4folate into acidic or hydrophobic solutions were used as references in determining the origin of the spectral changes seen as CH_3-H_4folate binds MetH(2−649). The CH_3-H_4folate spectrum at pH 3 is very similar to the spectrum previously reported for H_4folate at pH 3 (*38*). When CH_3-H_4folate is protonated at N5, a large shoulder appears at 264 nm and there is a decrease in absorption at 290 nm (Figure 5a). The spectra of CH_3-H_4-folate in increasing concentrations of acetonitrile were examined to determine changes in the spectrum of CH_3-H_4-folate upon transfer from an aqueous to a hydrophobic environment. When CH_3-H_4folate was transferred from aqueous solution to 80% acetonitrile and 20% AMT, pH 7.2, the spectrum was red-shifted, resulting in a difference spectrum (hydrophobic solvent − aqueous control) with an absorbance maximum at 306 nm and an extinction coefficient of 3800 M^{-1} cm^{-1} (Figure 4b). We also determined the absorbance changes associated with protonation of CH_3-H_4-folate in a more hydrophobic solvent, 80% acetonitrile and 20% AMT, pH 3, to establish the spectral changes expected

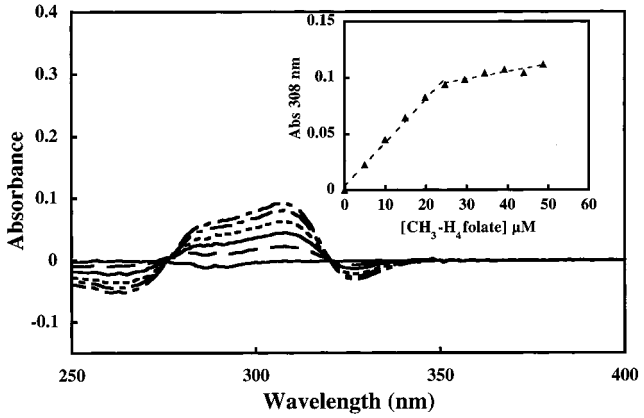

FIGURE 3: Difference spectra associated with CH_3-H_4folate binding to MetH(2−649) at pH 7.2. The initial trace, shown by the solid line with the lowest absorbance at 300 nm, is the difference spectrum seen before any substrate has been added and shows that equal concentrations of enzyme (20 μM) are in the front compartments of the sectored sample and reference Yankelev cuvettes. CH_3-H_4Folate was titrated into the front compartment of the sample cuvette and the rear compartment of the reference cuvette and spectra were measured after addition of 5, 10, 15, 20, and 25 μM CH_3-H_4folate. The absorbance increase at 308 nm was plotted versus CH_3-H_4folate concentration (inset). These data were fitted with the assumption of stoichiometric binding of CH_3-H_4folate to the enzyme during the initial phases of the titration. The slight absorbance increase at 308 nm after addition of 25 μM CH_3-H_4folate is an optical artifact seen at high αCH_3-H_4folate absorbances.

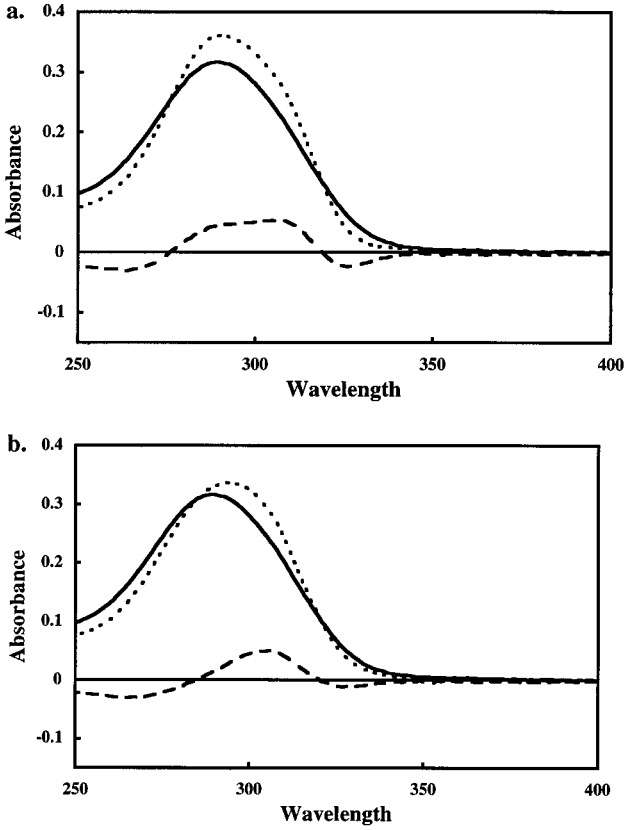

FIGURE 4: Comparison of UV/visible absorption changes associated with binding of CH_3-H_4folate to MetH(2−649) and on introduction of CH_3-H_4folate into 80% acetonitrile. The solid line in both panels represents the spectrum for 10 μM CH_3-H_4folate in AMT buffer, pH 7.2. (a) Absorbance changes associated with binding of CH_3-H_4folate to MetH(2−649). The dotted line is the absorbance spectrum obtained when 10 μM CH_3-H_4folate binds to an excess of MetH(2−649) after subtraction of the absorbance due to MetH-(2−649). The difference spectrum (bound - free CH_3-H_4folate) is indicated by the dashed line. This difference spectrum has an absorbance maximum at 308 nm with an extinction coefficient of 4300 M^{-1} s^{-1}. (b) Absorbance changes associated with introduction of an aqueous solution of CH_3-H_4folate into 80% acetonitrile. The dotted line shows the UV/visible absorption spectrum for CH_3-H_4-folate in 80% acetonitrile/20% AMT buffer, pH 7.2. The difference spectrum (acetonitrile - buffer) is shown by the dashed line and is characterized by an absorbance maximum at 306 nm with an extinction coefficient of 3800 M^{-1} s^{-1}.

for CH_3-H_4folate protonation while bound in a hydrophobic enzyme active site. Again, protonation is associated with increased absorbance at 264 nm and decreased absorbance at 290 nm (Figure 5b).

In summary, the difference spectrum observed for CH_3-H_4folate binding to MetH(2−649) at pH 7.2 most closely mimics the difference spectrum associated with transfer of CH_3-H_4folate into acetonitrile, consistent with the observed changes in the CH_3-H_4folate spectrum as it binds to MetH-(2−649) being due to transfer to a more hydrophobic environment. Furthermore, the spectral changes associated with protonation of free CH_3-H_4folate, in both aqueous and hydrophobic solutions, are opposite to the observed spectral changes at 264 and 308 nm associated with binding to the enzyme. From these data, it is clear that CH_3-H_4folate is not being protonated upon binding MetH(2−649) at pH 7.2.

H_4Folate binding to MetH(2−649) also resulted in similar changes in UV absorption, although the difference absorbance maximum was at 313 nm and the extinction coefficient was 5300 M^{-1} cm^{-1} (data not shown). The 15 nm red shift in the absorbance maximum associated with H_4folate binding to the enzyme (from 298 to 313 nm) is similar to the 18 nm red shift seen for CH_3-H_4folate binding (from 290 to 308 nm). These spectral changes can also be explained by H_4-folate moving from an aqueous environment to a more hydrophobic environment as it binds to MetH(2−649).

MetH(2−649) Preferentially Binds Unprotonated CH_3-H_4Folate. Measurements of the difference spectra associated with CH_3-H_4folate binding to MetH were made over the pH range where the enzyme is stable, from 5.4 to 9. Figure 6a shows the observed changes in the difference spectra for CH_3-H_4PteGlu$_3$ binding MetH(2−649) as the pH is lowered from pH 7.2 to 5.4. As the pH is lowered, the decrease in absorbance at 264 nm and the increase at 308 nm associated with binding of CH_3-H_4folate to MetH become even more prominent. Simulations of spectral changes were used in order to predict and explain the changes in UV spectra that were experimentally observed; the protocol for these simulations is described under Experimental Procedures. Figure 6b shows the predicted difference spectra at pH 5.4 and 5.7 calculated with the assumption that MetH(2−649) binds only unprotonated CH_3-H_4folate. The observed spectral changes in Figure 6a match the simulated spectra in Figure 6b quite well. The simulations reproduce the increased magnitude of the dip in the difference spectrum at 264 nm as the pH is lowered from pH 7.2 to 5.4. The change in absorbance at 264 nm was measured in the presence of saturating CH_3-H_4folate and MetH(2−649) for pH values from 5.3 to 9.0 and plotted versus pH in Figure 6c. The estimated pK_a of 5.1 closely matches the pK_a for N5 of CH_3-H_4folate. Such a decrease at 264 nm would be expected if there were a higher concentration of protonated CH_3-H_4folate in the reference

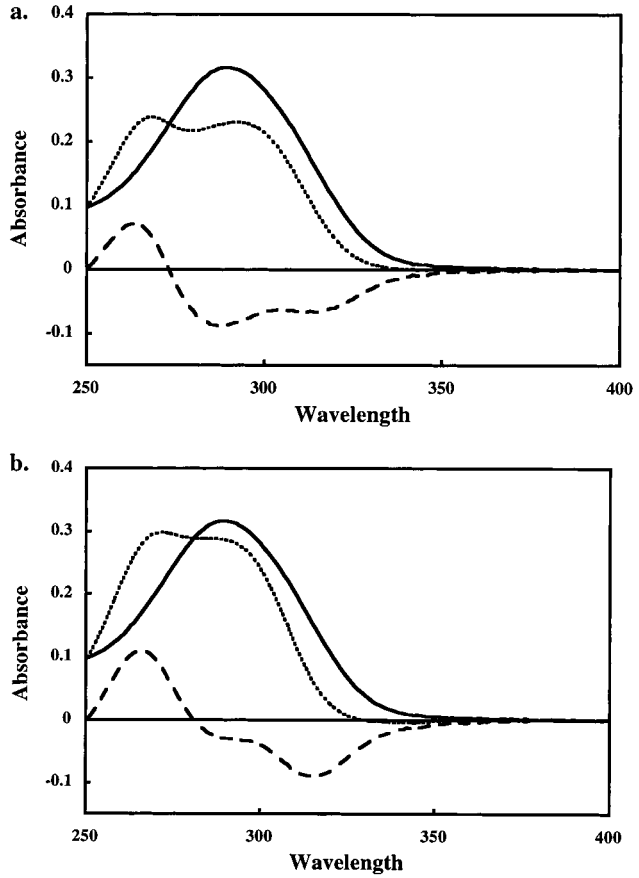

FIGURE 5: UV/visible absorption changes associated with protonation of CH_3-H_4folate in aqueous buffer (a) or in 80% acetonitrile (b). (a) The solid line shows the UV absorption spectrum for 10 μM CH_3-H_4folate in AMT buffer at pH 7.2. The dotted line shows the spectrum for CH_3-H_4folate in AMT buffer at pH 3; this spectrum is characterized by increased absorbance at 264 nm and decreased absorbance at 290 nm relative to the spectrum at pH 7.2. The dashed line shows the difference spectrum associated with protonation of CH_3-H_4folate in aqueous solution (3.0−7.2). (b) The solid line is the same as in panel a and shows the UV absorption spectrum for 10 μM CH_3-H_4folate in AMT buffer at pH 7.2. The dotted line shows the spectrum for CH_3-H_4folate in 80% acetonitrile and 20% AMT buffer, pH 3.0. This spectrum exhibits a prominent shoulder at 264 nm. The difference spectrum (pH 3.0, 80% acetonitrile − pH 7.2, aqueous) is shown with a dashed line. Note that the decrease in absorbance at 290 nm is much greater for protonation in aqueous solution than for protonation in 80% acetonitrile.

cuvette than in the sample cuvette, as would occur if MetH(2−649) preferentially bound unprotonated CH_3-H_4folate even at pH 5.3. This experiment indicates that binding of CH_3-H_4folate to MetH(2−649) is associated with a decrease in the pK_a for protonation at N5, as expected on transfer of this substrate into a hydrophobic environment.

Homology of MetH(353−649) to Dihydropteroate Synthase Indicates That the MetH Binding Site for CH_3-H_4Folate Is in a Hydrophobic Pocket in an $\alpha_8\beta_8$ Barrel. Significant homology between the microbial enzyme dihydropteroate synthase (DHPS) and the CH_3-H_4folate binding region of MetH (residues 353−649) has been found by use of the PSI-BLAST search program (*39*). PSI-BLAST gives a probability (*E* value) of 1.0×10^{-11} that MetH (353−649) and DHPS from *S. aureus* are related by chance. DHPS catalyzes the condensation of 6-hydroxymethyldihydropterin pyrophosphate and *p*-aminobenzoate to form dihydropteroate and pyrophosphate and thus shares with MetH(353−649) the

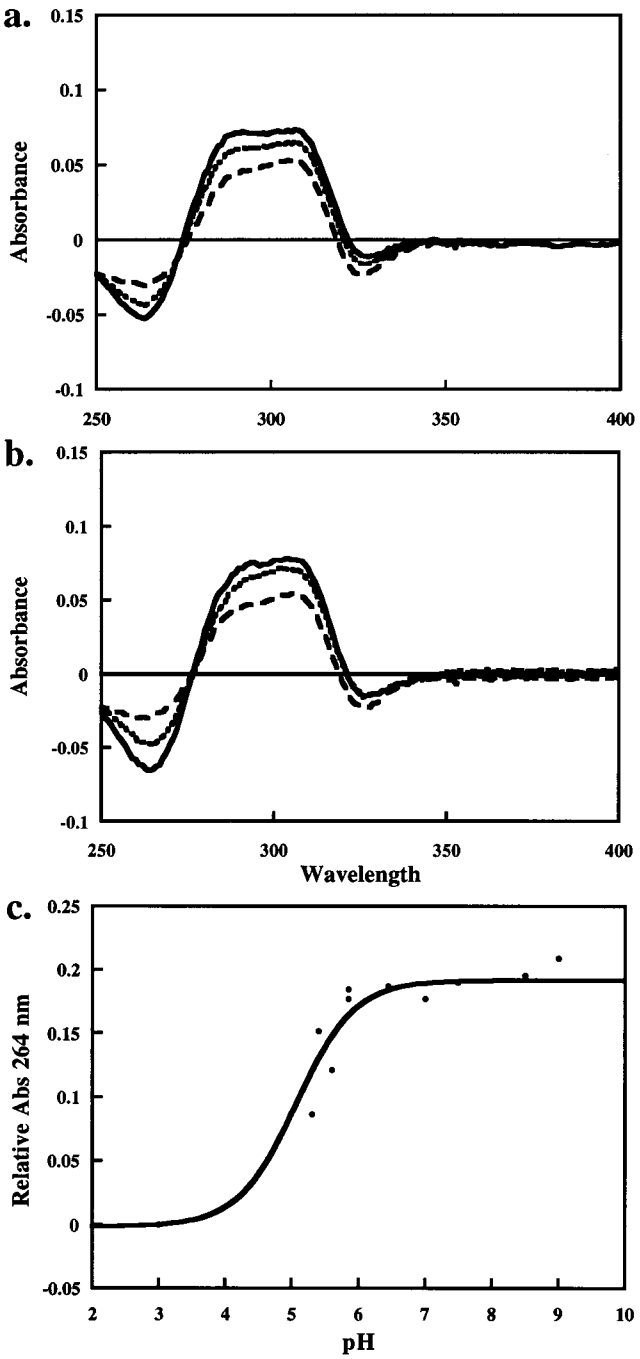

FIGURE 6: Comparison of observed and calculated difference spectra for binding of CH_3-H_4folate to MetH(2−649) as a function of pH. CH_3-H_4PteGlu$_3$ was used for these titrations, because it binds to MetH more tightly while exhibiting very similar absorbance changes. (a) Observed spectra: pH 7.2, dashed line; pH 5.7, dotted line; pH 5.4, solid line. (b) Calculated spectra. Experimentally observed difference spectrum for binding 12 μM CH_3-H_4PteGlu$_3$ to 10 mM MetH(2−649) in AMT buffer at pH 7.2 is shown (dashed line). At pH 5.7 (dotted line) and 5.4 (solid line), difference spectra have been calculated by assuming that only protonated CH_3-H_4PteGlu$_3$ binds to the enzyme, so that binding of CH_3-H_4PteGlu$_3$ is associated with spectral changes due to deprotonation of the substrate on binding. Details of calculations are presented under Experimental Procedures. (c) Plot of calculated decrease in absorbance at 264 nm associated with binding of CH_3-H_4folate to MetH(2−649) vs pH is shown (solid line), and observed changes in absorbance at 264 at each pH are shown with filled circles. In these experiments 70 μM CH_3-H_4PteGlu$_1$ was mixed with 20 μM MetH(2−649). Under these conditions the absorbance changes due to binding are nearly maximal, even at the lowest pH value. For the calculated absorbance changes we again assumed that only unprotonated CH_3-H_4folate binds to MetH.

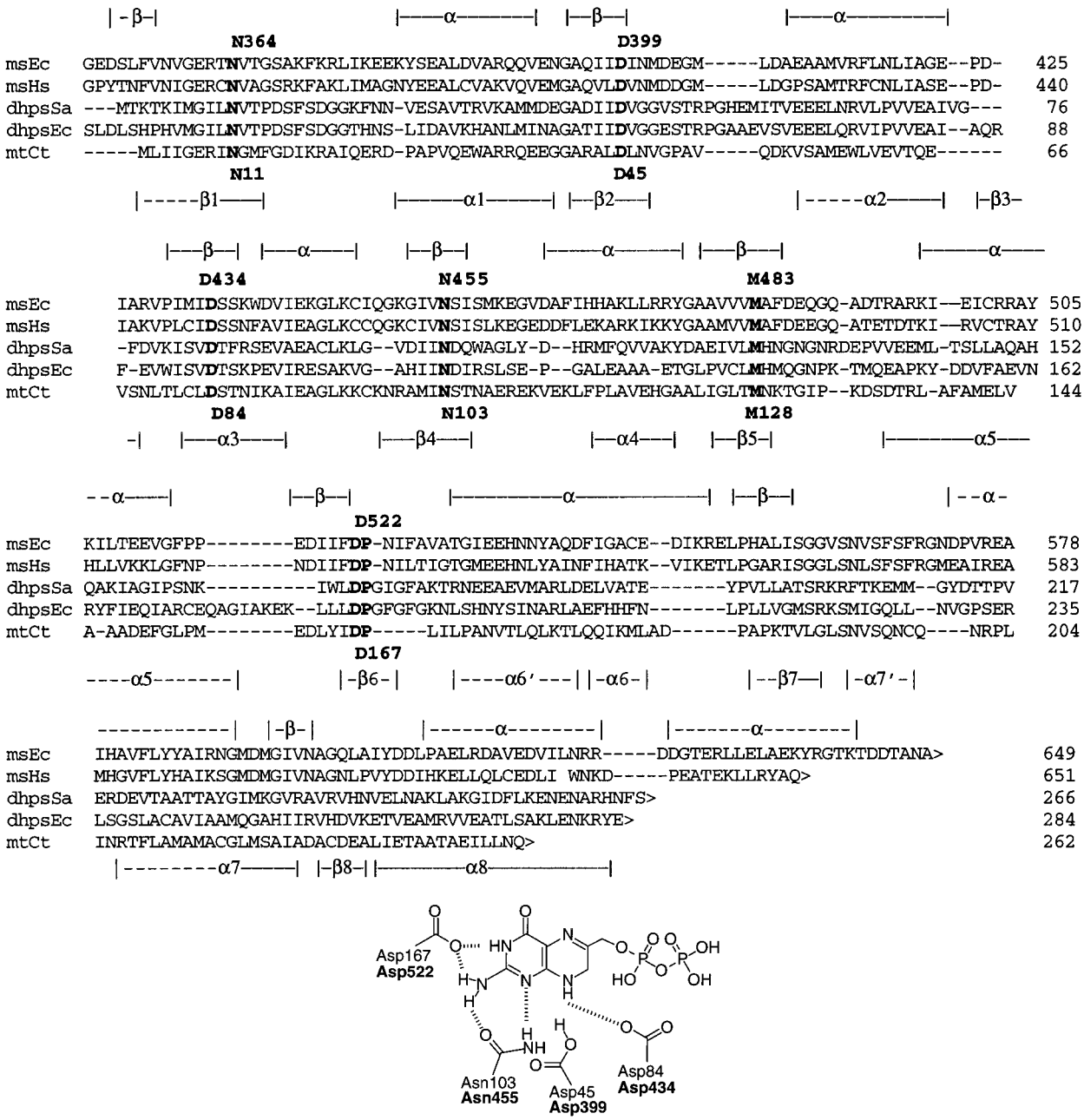

FIGURE 7: Sequence alignment of the CH_3-H_4folate-binding module of cobalamin-dependent methionine synthase with dihydropteroate synthase (DHPS), and AcsE by ClustalW *(40)*. From top to bottom the sequences shown are residues 353−649 of methionine synthase from *E. coli* (msEc), GenBank accession number J04975 *(28)*; residues 367−653 for methionine synthase from *Homo sapiens* (msHs), GenBank accession number NM_000254 *(56)*; DHPS from *S. aureus* (dhpsSa), GenBank accession number Z84573 *(41)*; DHPS from *E. coli* (dhpsEc), GenBank accession number X68777 *(57)*; and AcsE from *C. thermoaceticum* (mtCt), GenBank accession number L34780 *(5)*. The secondary structure prediction for *E. coli* MetH obtained by use of the PhD program *(43)* is shown above the top sequence, and the secondary structure determined from the *S. aureus* DHPS crystal structure *(41)* is shown below the bottom sequence in the alignment. α-Helices and *β*-strands are symbolized by their Greek letters. Residues shown in boldface type were identical in all the aligned sequences and those numbered were determined to be in the active site in both the *S. aureus* and *E. coli* DHPS crystal structures *(41, 42)*. The numbers on the top of the alignment correspond to residues in the *E. coli* MetH sequence, and the numbers on the bottom correspond to the corresponding residues in the *S. aureus* DHPS sequence. The crystal structure for AcsE from *C. thermoaceticum* MeTr has been recently solved and has been determined to be homologous to the DHPS crystal structures (*58*). Shown below the alignment is a cartoon of the amino acid hydrogen-bonding interactions with the DHPS substrate analogue HMPPP, as determined from the *S. aureus* DHPS crystal structure (Protein Data Bank file 1ad4) *(41)*. Conserved residues from *S. aureus* DHPS are numbered with plain text, with the corresponding residue numbers from *E. coli* MetH shown in boldface type below.

ability to bind pterin substrates. By use of ClustalW (*40*), seven MetH sequences, 12 DHPS sequences, and the AcsE methyltransferase sequence from *C. thermoaceticum* were aligned. A subset of these aligned sequences is shown in Figure 7. This alignment is particularly useful since crystal structures of DHPS enzymes from *Staphylococcus aureus* (*41*) and *E. coli* (*42*) have recently been solved. Although only seven residues are absolutely conserved in this alignment, the amino acids that are conserved are adjacent to the pterin ring in the DHPS crystal structures. The conserved aspartic acids Asp 84 and Asp 167 (in the numbering system for DHPS from *S. aureus*) shown in boldface type in the

Table 1: Properties of Wild-Type and Mutant MetH(2−649) Enzymes

MetH(2−649)	K_d for CH_3-H_4folate (μM)	K_m for CH_3-H_4folate (μM)	k_{cat}/K_m for cob(I)alamin[a] ($M^{-1}\,s^{-1}$)
wild type	9 ± 5	60	430
Asp399Asn	70 ± 20	200	9
Asp434Asn	15 ± 5	nd[b]	nd
Asp522Asn	>300	nd	nd

[a] The rate constant k_{obs} was determined by the CH_3-H_4folate:cob(I)alamin methyl transfer assay in the presence of saturating CH_3-H_4folate. The observed rate of methylcobalamin formation was divided by the concentration of MetH(2−649) and that of cob(I)alamin to obtain the second-order rate constant. [b] Not detectable.

alignment are involved in hydrogen bonding with the pterin ring of the DHPS substrate analogue, hydroxymethylpterin pyrophosphate, as also shown schematically in Figure 7. In addition, secondary structure predictions for the CH_3-H_4-folate-binding region of MetH (*43*) align with the known secondary structure of DHPS. DHPS binds its substrate in a hydrophobic active site in the center of an $\alpha_8\beta_8$ barrel, with the side chain at C6 projecting out of the center of the barrel. Recently, the crystal structure for AcsE was solved by Doukov et al., and this protein was also shown to be an $\alpha_8\beta_8$ barrel (*58*).

To probe the predicted homology to DHPS, each conserved aspartic acid residue shown in the alignment in Figure 7 was mutated to an asparagine residue in MetH(2−649). The mutant enzymes were analyzed for their ability to bind CH_3-H_4folate and to determine their catalytic activity (Table 1). Each mutant enzyme was fully active in the homocysteine:methylcobalamin methyltransferase assay. However, we found no detectable catalytic activity in the CH_3-H_4folate:cob(I)alamin methyltransferase assay for Asp434Asn MetH(2−649) and Asp522Asn MetH(2−649) and a 40-fold reduction in activity for Asp399Asn MetH(2−649). When these mutants were analyzed for their ability to bind CH_3-H_4folate, a drastic reduction in binding affinity was seen in Asp522Asn MetH(2−649); no binding could be detected and the K_d for CH_3-H_4folate was determined to be >300 μM. An 8-fold decrease in affinity for CH_3-H_4folate was observed for the Asp399Asn mutation. The properties of the mutant enzymes support the notion that the pterin ring of CH_3-H_4-folate binds the folate-activating module of MetH in an orientation that resembles that of the pterin ring of DHPS. One of the seven conserved residues in the alignment of DHPS and MetH is Met128 of DHPS from *S. aureus*, which makes a hydrophobic contact with the pterin ring (*42*). Thus, we expect binding of CH_3-H_4folate to MetH to result in absorbance changes characteristic of transfer of CH_3-H_4folate to a more hydrophobic environment and in a lowered pK_a for protonation at N5.

DISCUSSION

In this paper, we describe experiments to probe the role of methionine synthase in activating CH_3-H_4folate for participation in methyl transfer reactions. Two modes of ground-state activation of CH_3-H_4folate can be envisioned. The methyl group is formally transferred as a carbocation. Protonation at either the N5 or C8a position of the tetrahydropterin ring could serve to labilize the methyl group by providing the tetrahydropterin with an "electron sink" to accept the electrons from the N5−methyl bond. Alternatively, either one- or two-electron oxidation of CH_3-H_4folate could activate CH_3-H_4folate for participation in the methyl transfer reaction. In other words, protonation or oxidation to form an aminium or iminium cation at N5 could facilitate the reaction. Methyl transfers from the aminium cation 5,5-dimethyltetrahydropterin to cob(I)alamin have been documented, but these methyl transfers occurred in low yield (*22*).

Our studies suggest that activation of CH_3-H_4folate does not occur in the ground-state binary complex with MetH(2−649). CH_3-H_4folate is not protonated in the binary complex with MetH(2−649) throughout the pH range where the enzyme is stable. It is also clear from these studies that CH_3-H_4folate is not activated by oxidation in the binary enzyme−CH_3-H_4folate complex. Oxidation would also lead to distinctive changes in the UV−visible absorption spectrum. For instance, two-electron oxidation of CH_3-H_4folate to 5-methyl-7,8-dihydrofolate is associated with a blue shift in the absorbance maximum (*44*). Alternatively, oxidation to quininoid 5-methyldihydrofolate is associated with a slight red shift, as seen here, but also with a significant decrease in the molar extinction coefficient (*45*), which is the opposite of the spectral changes observed in our experiments. An interpretation that is consistent with our current data is that CH_3-H_4folate is introduced into a more hydrophobic environment on binding to the protein, which would be expected to lower the pK_a associated with protonation of N5. The crystal structure of DHPS, which is homologous to the CH_3-H_4-folate-binding module of MetH, is consistent with our interpretation of the binding environment of CH_3-H_4folate in MetH.

Our experiments do not exclude the possiblity that protonation of CH_3-H_4folate occurs only in the ternary complex with cob(I)alamin, but we know of no precedent for an S_N2 reaction in which group transfer is concerted with proton transfer. We are therefore driven to propose an alternate mechanism for methyl transfer to cob(I)alamin enzymes.

In methanogenic Archaea, a wide variety of compounds serve as methyl donors to corrinoid proteins, including methanol, mono-, di-, and trimethylamines, dimethyl sulfide, and chloromethane (*9, 46*−*50*). In these systems, activation by ground-state protonation of the methyl donors is not appealing, because the pK_a values for protonation of these methyl donors range as low as −1.5 for methanol. An attractive mechanism for methyl transfer in MetH(2−649) would also be applicable to all of these methyl donors.

A possible mechanism for methyl transfer from CH_3-H_4-folate is shown in Figure 8. This mechanism does not require protonation or oxidation of CH_3-H_4folate in the binary enzyme−substrate complex and might be applicable to all of the substrates that serve as methyl donors to cobalamin. In this oxidative addition mechanism, the cob(I)alamin cofactor is proposed to form a three-centered bond with enzyme-bound methyltetrahydrofolate: the empty 4s orbital of the cobalt hybridizes with the σ orbital of the N5−methyl bond, while the occupied $3d_{xz}$ or $3d_{yz}$ orbital of the cobalt hybridizes with the symmetry-matched σ^* orbital of the N5−methyl bond. These interactions would weaken the N5−methyl bond of CH_3-H_4folate, and the cobalt would serve as a Lewis acid to stabilize the H_4folate leaving group.

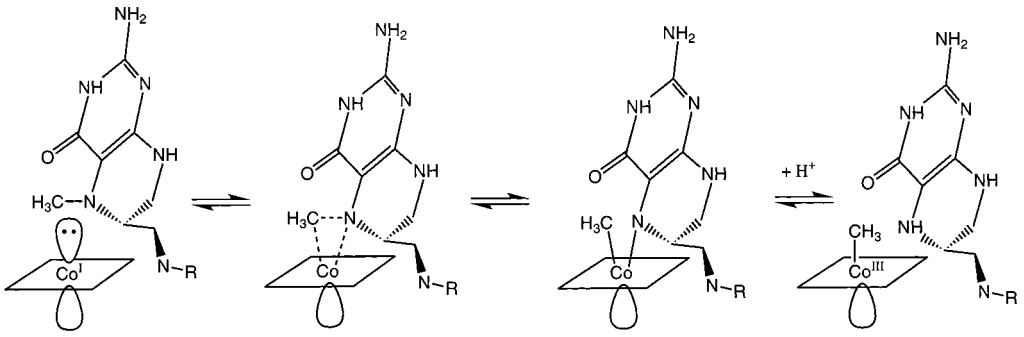

FIGURE 8: Proposed mechanism for oxidative addition of cob(I)alamin to the N5−methyl bond of CH_3-H_4folate.

Salient features of this proposal are the parallel orientation of the N−C bond of CH_3-H_4folate with the plane of the corrin ring, and the requirement for dissociation of the lower axial ligand to permit cis addition of tetrahydrofolate to the upper face of methylcobalamin in the reverse direction. In this context, the fact that AcsD lacks a lower axial ligand, while the lower axial ligand in MetH, MtrA, and CmuB is a histidine rather than dimethylbenzimidazole, may suggest that ligand replacement facilitates the dissociation of the lower axial ligand to allow cis addition to the upper face of the corrin. Crystal structures of complexes in which CH_3-H_4-folate is positioned for productive interaction would be of great interest because they should reveal the N−CH_3−Co bond angle.

Methyl transfer by an oxidative addition mechanism would be expected to occur with retention of configuration at the transferred methyl group (*51*). Our earlier observation that the methionine synthase reaction occurs with overall retention of stereochemistry in the transfer from CH_3-H_4folate to homocysteine (*18*) would then require that methyl transfer from methylcobalamin to homocysteine also occur with retention of stereochemistry, presumably also by an oxidative addition mechanism. Alkylation of cob(I)alamin by quaternary ammonium salts has been proposed as a model for the methionine synthase-catalyzed methyl transfer from CH_3-H_4folate to homocysteine (*21, 22*), and cob(I)alamin is methylated by 5,5-dimethyltetrahydropterin in low yield (*21*). The reactions of cobalamin with quaternary ammonium salts are inhibited by bulky substituents, suggesting that they proceed by S_N2 mechanisms. One may now question whether such reactions are indeed appropriate models for the enzyme-catalyzed reaction.

Our proposed mechanism has precedence in the oxidative addition to the N−H bond of ammonia observed with Co^{1+} in the gas phase (*52*), where a transient $[H-Co-NH_2]^{1+}$ adduct can be detected by guided ion beam mass spectrometry. The bond between nitrogen and cobalt in this intermediate is surprisingly strong, with an estimated bond dissociation energy of 62 kcal/mol, and further decomposition of this intermediate by expulsion of $^{\bullet}NH_2^-$ only occurs at very high energies. In proposing similar mechanisms of oxidative addition for gas-phase cobalt(I) and for cobalamin, one must of course be concerned about steric problems that might be encountered in forming a three-centered bond between the C−N of CH_3-H_4folate and the cobalt of cobalamin. It is not clear whether the dissociation of the lower ligand could permit the cobalt to move out of the plane defined by the equatorial ligands contributed by the corrin ring or whether the corrin ring could distort to reduce steric hindrance between its substituents and CH_3-H_4folate. However, observations of Silverman and Dolphin (*54*) are encouraging in this respect. These authors obtained evidence for formation of π complexes between cob(III)alamins and olefins as intermediates in cobalamin-catalyzed solvolysis reactions, suggesting that the corrin ring can distort sufficiently to form cis complexes.

The transition state for methyl transfer from CH_3-H_4folate to homocysteine may occur after N−C bond cleavage and require partial proton transfer to the NR_2 leaving group. Since the pK_a of the coordinated NR_2^- should increase drastically as the N−C bond is cleaved, protonation by a general acid catalyst on the enzyme may occur by the "libido effect" (*53*); namely, proton transfer would occur spontaneously at that point in the reaction sequence where the pK_a of N5 of H_4-folate becomes greater than the pK_a of the general acid catalyst.

Ragsdale and his colleagues (*24*) have conducted extensive kinetic analysis of the methyl transfer between CH_3-H_4folate and exogenous cob(I)alamin catalyzed by AcsE. These studies demonstrate that k_{cat} for methyl transfer increases as the pH is lowered from 8.4 to 6.3. At pH 8.4, k_{cat} approaches 0, while at 6.3, k_{cat} approaches 1.5 s^{-1}, and the data can be fit to an apparent pK_a of 7.0. Similar profiles were observed for the reaction between CH_3-H_4folate and the corrinoid of AcsD catalyzed by AcsE. Thus their results provide strong evidence for proton transfer in the transition state of the methyl transfer catalyzed by AcsE.

More recent studies on AcsE from the Ragsdale group (*55*) have used ^{13}C NMR to probe the protonation state of (6*R*,*S*)-[*methyl*-^{13}C]CH_3-H_4folate on binding to AcsE. When CH_3-H_4folate binds to AcsE, the resonance of the methyl carbon broadens and shifts downfield approximately 0.7 ppm as the pH is lowered from 7.6 to 5.1, with an apparent pK_a of 6.28 ± 0.08. This shift is small compared with the 2.4 ppm downfield shift observed on protonation of CH_3-H_4folate in solution, as determined in our studies and in their experiments (*55*). Although they interpreted their data as indicating protonation of bound CH_3-H_4folate, the small chemical shift might also reflect hydrogen-bond donation to the pterin on binding to the enzyme.

No proton uptake is associated with CH_3-H_4folate binding AcsE at pH 7.6 (*55*), nor do we see proton uptake when CH_3-H_4folate binds MetH(2−649) at pH 7.6 (*32*). As the pH is lowered, increasing proton uptake is associated with CH_3-H_4folate binding to AcsE until 0.84 equiv of protons is taken up on binding at pH 5.2 (*55*). However, the K_d for CH_3-H_4folate binding to AcsE is independent of pH over

the pH range from 5.5 to 7.0 (*55*), an observation that conflicts with their proton uptake measurements.

The proposed oxidative addition mechanism for the CH_3-H_4folate:cob(I)alamin methyl transfer reaction catalyzed by MetH is consistent with the data presented here and with much of the mechanistic data for AcsE. This mechanism also provides a common mechanism for cob(I)alamin methyl transfer enzymes that utilize methanol or methylamines as substrates. In the case of methanol, oxidative addition would produce hydroxide coordinated to the cobalt and thus neatly avoid the necessity of protonating methanol, with a pK_a of −1.5. The results of ongoing structural and kinetic studies of MetH and other corrinoid methyltransferases will be important in probing this proposed mechanism.

ACKNOWLEDGMENT

We thank Peter Armentrout and Richard Finke for helpful discussions and Sanmitra Deo for construction of the Asp399Asn MetH(2−649) and Asp522Asn MetH(2−649) expression plasmids.

REFERENCES

1. Banerjee, R. V., Frasca, V., Ballou, D. P., and Matthews, R. G. (1990) *Biochemistry 29*, 11101−11109.
2. Goulding, C. W., Postigo, D., and Matthews, R. G. (1997) *Biochemistry 36*, 8082−8091.
3. Goulding, C. W., and Matthews, R. G. (1997) *Biochemistry 36*, 15749−15757.
4. Garrow, T. A. (1996) *J. Biol. Chem. 271*, 22831−22838.
5. Roberts, D. L., Zhao, S., Doukov, T., and Ragsdale, S. W. (1994) *J. Bacteriol. 176*, 6127−6130.
6. Hu, S.-I., Pezacka, E., and Wood, H. G. (1884) *J. Biol. Chem. 259*, 8892−8897.
7. Ragsdale, S. W., Lindahl, P. A., and Munck, E. (1987) *J. Biol. Chem. 262*, 14289−14297.
8. Gartner, P., Weiss, D. S., Harms, U., and Thauer, R. K. (1994) *Eur. J. Biochem. 226*, 465−472.
9. Vanelli, T., Messmer, M., Studer, A., Vuilleumier, S., and Leisinger, T. (1999) *Proc. Natl. Acad. Sci. U.S.A. 96*, 4615−4620.
10. Hippler, B., and Thauer, R. K. (1999) *FEBS Lett. 449*, 165−168.
11. Studer, A., Vuilleumier, S., and Leisinger, T. (1999) *Eur. J. Biochem. 264*, 242−249.
12. Drennan, C. L., Huang, S., Drummond, J. T., Matthews, R. G., and Ludwig, M. L. (1994) *Science 266*, 1669−1674.
13. Wirt, M. D., Kumar, M., Ragsdale, S. W., and Chance, M. R. (1993) *J. Am. Chem. Soc. 115*, 2146−2150.
14. Harms, U., and Thauer, R. K. (1996) *Eur. J. Biochem. 241*, 149−154.
15. Drummon, J. T., Huang, S., Blumenthal, R. M., and Matthews, R. G. (1993) *Biochemistry 32*, 9290−9295.
16. Fujii, K., and Huennekens, F. M. (1979) in *Biochemical Aspects of Nutrition* (Yagi, K., Ed.) pp 173−184, University Park Press, Baltimore, MD.
17. Luschinsky, C. L., Drummond, J. T., and Matthews, R. G. (1992) *J. Mol. Biol. 225*, 557−560.
18. Zydowsky, T. M., Courtney, L. F., Frasca, V., Kobayashi, K., Shimizu, H., Yuen, L.-D., Matthews, R. G., Benkovic, S. J., and Floss, H. G. (1986) *J. Am. Chem. Soc. 108*, 3152−3153.
19. Schrauzer, G. N., and Deutsch, E. (1969) *J. Am. Chem. Soc. 91*, 3341−3350.
20. Brown, K. L. (1982) in *B_{12}* (Dolphin, D., Ed.) pp 245−294, Wiley-Interscience, New York.
21. Hilhorst, E., Iskander, A. S., Chen, T., and Pandit, U. K. (1993) *Tetrahedron Lett. 34*, 4257−4260.
22. Hilhorst, E., Iskander, A. S., Chen, T., and Pandit, U. K. (1994) *Tetrahedron 50*, 8863−8870.
23. Taylor, R. T., and Hanna, M. L. (1972) *Arch. Biochem. Biophys. 151*, 401−413.
24. Zhao, S., Roberts, D. L., and Ragsdale, S. W. (1995) *Biochemistry 34*, 15075−15083.
25. Matthews, R. G. (1986) *Methods Enzymol. 122*, 333−339.
26. Mathews, C. K., and Heunnekens, F. M. (1963) *J. Biol. Chem. 238*, 3436.
27. Blakely, R. L. (1960) *Nature 188*, 231−232.
28. Banerjee, R. V., Johnston, N. L., Sobeski, J. K., Datta, P., and Matthews, R. G. (1989) *J. Biol. Chem. 264*, 13888−13895.
29. Jarrett, J. T., Goulding, C. G., Fluhr, K., Huang, S., and Matthews, R. G. (1997) *Methods Enzymol. 281*, 196−213.
30. Doddrell, D. M., Pegg, D. T., and Bendall, M. R. (1982) *J. Magn. Reson. 48*, 323.
31. Langsetmo, K., Fuchs, J. A., and Woodward, C. (1991) *Biochemistry 30*, 7603−7609.
32. Jarrett, J. T., Choi, C. Y., and Matthews, R. G. (1997) *Biochemistry 36*, 15739−15748.
33. Ellis, K. J., and Morrison, J. F. (1982) *Methods Enzymol. 87*, 405−426.
34. Zhou, Z. S., Peariso, K., Penner-Hahn, J. E., and Matthews, R. G. (1999) *Biochemistry 38*, 15915−15926.
35. Segel, I. H. (1975) *Enzyme Kinetics: Behavior and Analysis of Rapid Equilibrium and Steady-State Enzyme Systems*, John Wiley and Sons, New York.
36. Whiteley, J. M., and Russell, A. (1981) *Biochem. Biophys. Res. Commun. 101*, 1259−1265.
37. Breitmaier, E. (1993) *Structure elucidation by NMR in organic chemistry: a practical guide*; Wiley, Chichester, England, and New York.
38. Kallen, R. G., and Jencks, W. P. (1966) *J. Biol. Chem. 241*, 5845−5846.
39. Altschul, S. F., Madden, T. L., Schaffer, A. A., Zhang, J., Zhang, Z., Miller, W., and Lipman, D. J. (1997) *Nucleic Acids Res. 25*, 3389−3402.
40. Thompson, J. D., and Higgins, D. G. (1994) *Nucleic Acids Res. 22*, 4673−4680.
41. Hampele, I. C., D'Arcy, A., Dale, G. E., Kostrewa, K., Nielsen, J., Oefner, C., Page, M. G. P., Schonfeld, H., Stuber, D., and Then, R. L. (1997) *J. Mol. Biol. 268*, 21−30.
42. Achari, A., Somers, D. O., Champness, J. N., Bryant, P. K., Rosemond, J., and Stammers, D. K. (1997) *Nat. Struct. Biol. 4*, 490−497.
43. Rost, B. (1996) *Methods Enzymol. 266*, 525−539.
44. Kaufman, S. (1967) *J. Biol. Chem. 242*, 3934−3943.
45. Davis, M. D., and Kaufman, S. (1989) *J. Biol. Chem. 264*, 8585−8596.
46. Daas, P. J. H., Hagen, W. R., Keltjens, J. T., van der Drift, C., and Vogels, G. D. (1996) *J. Biol. Chem. 271*, 22346−22351.
47. Sauer, K., and Thauer, R. (1999) *Eur. J. Biochem. 261*, 674−681.
48. Burke, S. A., and Krzycki, J. A. (1997) *J. Biol. Chem. 272*, 16570−16577.
49. Ferguson, D. J. J., and Krzycki, J. A. (1997) *J. Bacteriol. 179*, 846−852.
50. Tallant, T. C., and Krzycki, J. A. (1997) *J. Bacteriol. 179*, 6902−6911.
51. Collman, J. P., Hegedus, L. S., Norton, J. R., and Finke, R. G. (1987) *Principles and applications of organotransition metal chemistry*, University Science Books, Sausalito, CA.
52. Clemmer, D. E., and Armentrout, P. B. (1989) *J. Am. Chem. Soc. 111*, 8280−8281.
53. Jencks, W. P. (1972) *J. Am. Chem. Soc. 94*, 4731−4732.
54. Silverman, R. B., and Dolphin, D. (1976) *J. Am. Chem. Soc. 98*, 4626−4633.
55. Seravalli, J., Shoemaker, R. K., Sudbeck, M. J., and Ragsdale, S. W. (1999) *Biochemistry 38*, 5736−5745.
56. Li, Y. N., Gulati, S., Baker, P. J., Brody, L. C., Banerjee, R., and Kruger, W. D. (1996) *Hum. Mol. Genet. 5*, 1851−1858.
57. Swedberg, G., Fermer, C., and Skold, O. (1993) *Adv. Exp. Med. Biol. 338*, 555−558.
58. Doukov, T., Seravalli, J., Stezowski, J. J., and Ragsdale, S. W. (2000) *Structure 8*, 817−830.

BI001431X